Thick Supercritical Airfoils with Low Drag and Natural Laminar Flow

B. Eggleston* and R.J.D. Poole†
de Havilland Aircraft Company of Canada, Downsview, Ontario, Canada
D.J. Jones‡ and M. Khalid§
National Research Council of Canada, Ottawa, Ontario, Canada

A family of natural laminar flow-capable, supercritical airfoils has been designed to have good characteristics with turbulent flow while being capable of supporting up to 70% chord natural laminar flow in favorable conditions. Tests are reported on airfoils of 16 and 21% chord maximum thicknesses in NAE 15×60 in. two-dimensional wind tunnel. At Reynolds numbers up to 10 million and over a narrow range of Mach numbers close to their design conditions, the airfoils supported extensive runs of laminar flow and their drag was reduced more than 50% relative to values with turbulent boundary layers. At higher Reynolds numbers, the natural laminar flow capability diminished rapidly due to various factors. The airfoil cruise drag characteristics at all Reynolds numbers tested (8–20 million) were markedly superior to airfoils of similar thickness tested previously in the same facility.

Nomenclature

c	= airfoil chord
C_L	= lift coefficient
$C_{L\mathrm{des}}$	= design lift coefficient
C_D	= drag coefficient
$C_{D\min}$	= minimum drag coefficient
C_M	= pitching moment coefficient
H	= boundary layer shape factor
M	= Mach number
M_{des}	= design Mach number
M_{dr}	= drag rise Mach number
Re	= Reynolds number
Re_c	= chord-based Reynolds number
Re_{tr}	= Reynolds number based on transition distance
t/c	= maximum thickness/chord ratio
x	= chordwise location from leading edge, positive aft

Introduction

FUTURE transport aircraft will benefit from improved airfoil designs that reduce wing section drag. Toward that objective, the de Havilland Aircraft Company of Canada and the National Aeronautical Establishment of the National Research Council of Canada have an ongoing program of research and development aimed at developing improved supercritical airfoils suitable for future regional transport aircraft. These airfoils will possibly use some form of advanced propellers to cruise at high subsonic speeds. The purpose of this paper is to present some experimental results for new designs of thick supercritical airfoils that are capable of supporting extensive regions of natural laminar flow (NLF) in suitably favorable conditions. This technology will provide substantial reductions in drag or alternatively allow substantial increases in wing thickness for a given design Mach number and lift coefficient.

Received Sept. 26, 1986; revision received Dec. 2, 1986.

*Manager Advanced Design.

†Senior Research Engineer.

‡Senior Research Officer, National Aeronautical Establishment. Member AIAA.

§Associate Research Officer, National Aeronautical Establishment.

When designing these airfoils, one of the foremost objectives was to ensure that good aerodynamic characteristics were retained when the boundary layers were made turbulent from near the noses of the airfoils. This situation can be expected to prevail frequently, for premature transition can often be caused by some type of surface contamination or freestream turbulence. However, in circumstances where conditions are sufficiently "clean" the natural laminar flow (NLF)-capable airfoils can support laminar flow back to 60–70% chord on their upper surfaces and up to 50% chord on their lower surfaces. This extent of laminar flow will lead to drag reductions of at least 50% relative to the same airfoils with turbulent boundary layers.

Validating the performance of NLF-capable airfoils at high Reynolds numbers becomes difficult in wind tunnels due to the need for very low turbulence levels and for extremely fine tolerances on small models. Measurements made in 1978 by Elfstrom in the NAE 15×60 in. wind tunnel[1] showed turbulence levels were about 0.3% at Reynolds numbers of 14–20 million. Calculations made using this level of turbulence with the method of Van Driest and Blumer[2] suggested there was little prospect for extensive NLF under these conditions. However, subsequent tests[3] showed evidence of NLF back to 40% chord on an airfoil with a flat pressure distribution at a Reynolds number of 14 million. As a consequence, at the outset of this investigation the prospects for achieving extensive NLF were uncertain. This points out the need for further measurements of tunnel turbulence and, on the theoretical side, the development of more reliable criteria for predicting transition.

Two airfoils were designed and tested at 16 and 21% chord maximum thickness and their geometries are shown in Fig. 1. A summary of the design conditions for the airfoils is given in Table 1. The table also includes estimates of the drag rise Mach numbers with turbulent boundary layers, which were made at high Reynolds numbers using an extended version of the BGK code of Ref. 4. The design lift coefficient $C_{L\mathrm{des}}$ selected for the airfoils was 0.6 to suit aircraft operating over long ranges and at high altitudes. It is noted that the selected $C_{L\mathrm{des}}$ is much higher than considered in Ref. 5 where a value of 0.35 was utilized and lower camber airfoils resulted.

Some features of the design velocity distribution for the 16% t/c airfoil are summarized in Fig. 2. At the design condition the peak Mach numbers on the upper surface were kept to 1.10–1.12 to give low wave drag, and the velocity gradients were made slightly favorable to encourage NLF. A moderate amount of aft loading was used to enhance performance, subject to the constraint that pitching moment coefficients should not be less than −0.14 at the design condition. Boundary-layer calculations were made with fully turbulent conditions which showed good margins from flow separation on the upper and lower surfaces of both airfoils at their respective design conditions. Although Fig. 10 shows the shape factor H close to separation values near the trailing edge, experience suggested this extent was not serious and it would be relieved in the tests to give attachment.

The airfoils were tested in the NRC/NAE 15×60 in. two-dimensional wind tunnel over a range of Reynolds numbers of 8 to 20 million/ft. The tunnel is a blowdown type with the top and bottom walls having holes giving a porosity of 20.5%, and the sidewalls having controlled suction in the region of the model. Further details on the wind tunnel can be found in Ref. 6. The model of the 16% t/c airfoil was made of 12 in. chord and the model of the 21% t/c airfoil was of 10 in. chord. The remainder of this paper will review selected results from tests of the 16% and 21% thick airfoils, concentrating mainly on the airfoil drag characteristics. Further information on the tests of the 21% thick airfoil are given in Ref. 7. Other NLF airfoils of 10% and 13% thicknesses have also been designed and tests are planned in early 1987 to complete the investigations.

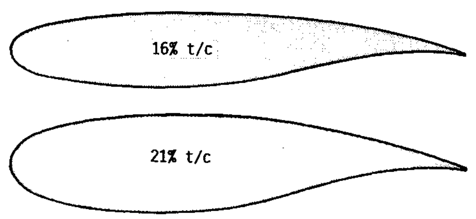

Fig. 1 DHC-NRC thick supercritical airfoils.

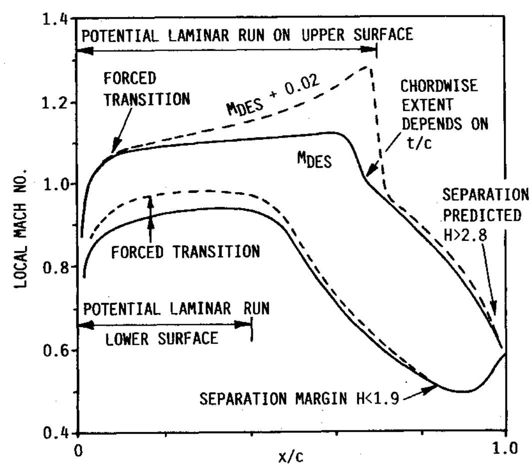

Fig. 2 Features of design pressure distributions based on BGK (extended) predictions.

Flow Visualization

The flow visualization was obtained by spraying the airfoils with a thin film of oil containing a dye which fluoresced in ultraviolet light. The application required some care as a film that was too thick could cause premature transition which would alter the airfoil aerodynamic characteristics markedly at low Reynolds numbers.

Photographs of flow visualization results for the 16% thick airfoil at a lift coefficient of 0.6 and Mach numbers about 0.75, for several Reynolds numbers are shown in Figs. 3 and 4. At a chord Reynolds number Re_c of 8 million, most of the upper surface repeatedly sustained laminar flow back to 70% chord which coincided with the shock location. The disturbances due to the pressure taps caused a transition wedge of sufficient spanwise extent to influence the centerline probe of the wake traverse apparatus. Although the models were cleaned very thoroughly between runs to remove any contamination, the flow visualization showed a few isolated transition wedges due to minute particles from tunnel contamination during the run, and they were distributed haphazardly over the surface.

Increasing the Re_c to 14 million reduced the extent of the NLF to 45% chord at the very most on the upper surface, Fig. 4. The laminar region became very patchy and transition even originated at the leading edge in several places. The further increase of Re_c to 20 million reduced the NLF to 20% chord at the most, but the spanwise extent of the coverage was so sparse that the airfoil was essentially fully turbulent in behavior, Fig. 4.

The corresponding flow visualization results for the lower surface at Re_c of 8–20 million are shown in Fig. 5. The model featured a detachable bottom plate held in place by

Table 1 Airfoil design conditions

	t/c, %	
	16	21
M_{des}	0.72	0.68
C_{Ldes}	0.6	0.6
M_{dr}[a]	0.75	0.70

[a]From Ref. 4, with $Re_c = 20$ million.

1 TRANSITION WEDGE DUE TO LINE OF PRESSURE TAPS
2 TRANSITION WEDGES DUE TO TO SPECKS OF DIRT
3 LAMINAR RUN BACK TO 70% CHORD
4 TURBULENT FLOW IN PRESSURE RECOVERY REGION
5 SHOCK LOCATION IN TURBULENT FLOW
6 PRESSURE TAPPINGS OFFSET TO REDUCE EFFECTS OF TRANSITION ON PROBE No 1

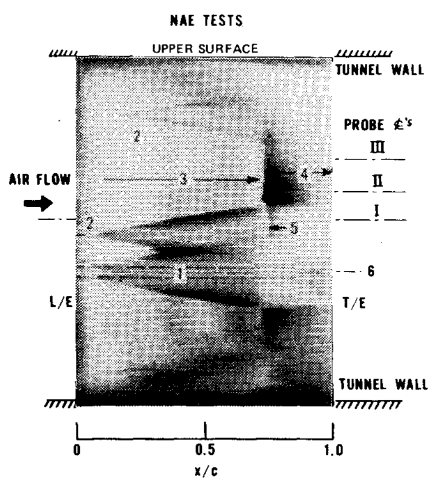

Fig. 3 Flow visualization at $Re = 8$ million; $M = 0.75$, and $C_L = 0.6$.

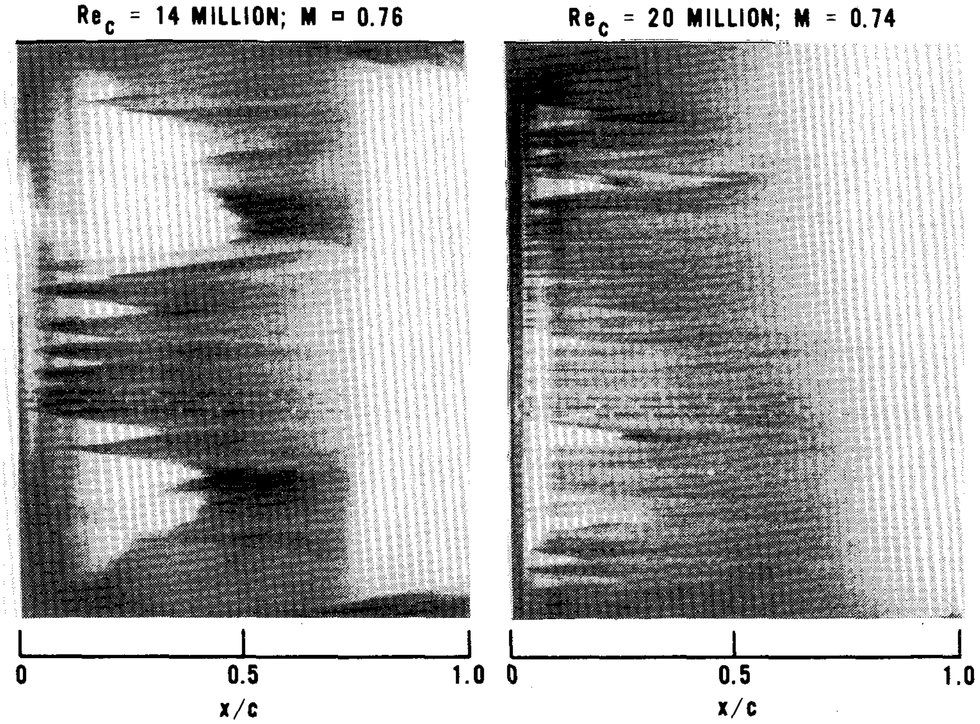

Fig. 4 Sixteen percent airfoil flow visualization on upper surface transition free; $C_L = 0.6$.

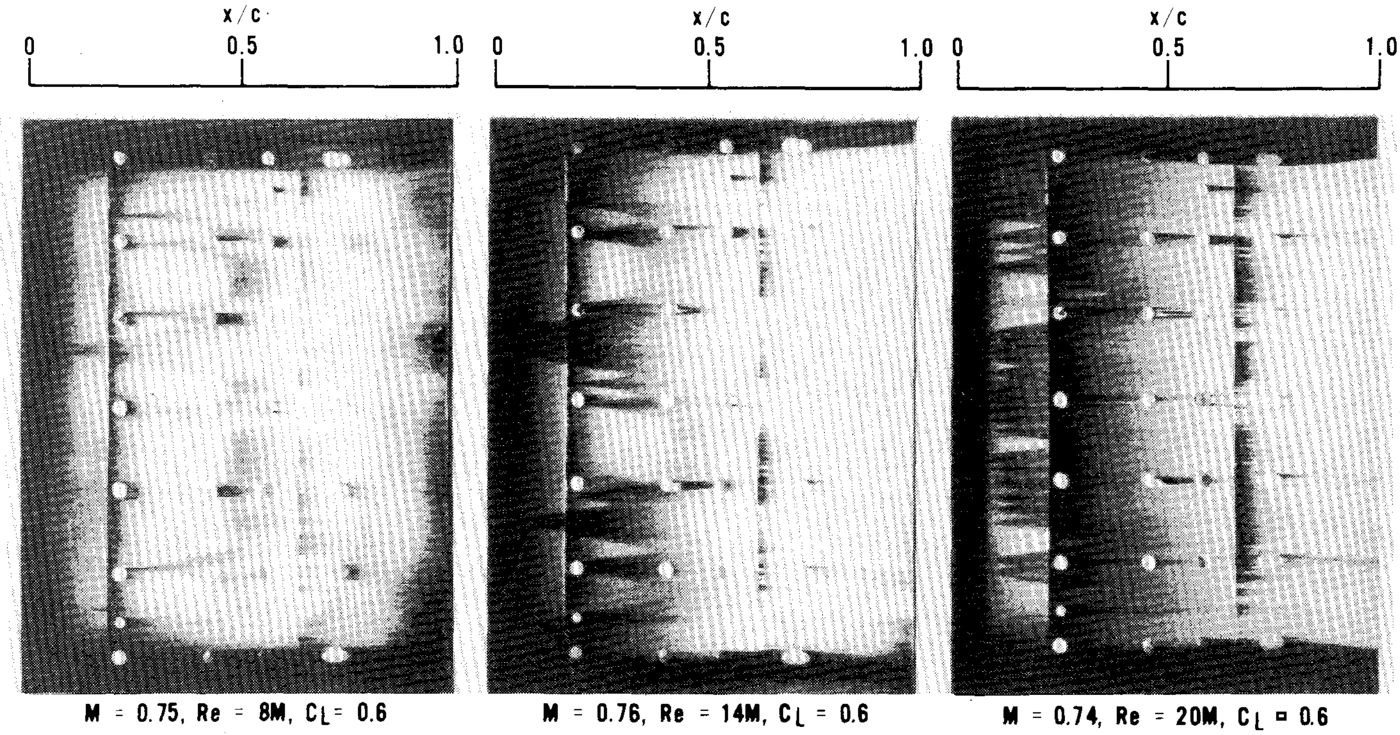

Fig. 5 Flow visualization, wing lower surface.

screws and although the screw holes were filled carefully they still caused sufficient disturbance to trigger transition. The lower surface supported NLF to 50% chord between the holes but the reduced spanwise coverage would result in a significant drag increase.

The chordwise location of transition on the 16% airfoil is shown as a function of Re_c in Fig. 6, as derived from the longest runs of NLF observed on each surface at a lift coefficient of 0.6 and Mach numbers of about 0.75. Basing the Reynolds number on the transition distance showed that the Re_{tr} on the upper surface was roughly 6 million for chord based Re up to 12 million, but thereafter Re_{tr} reduced rapidly to about 4 million at the highest test Reynolds number. Also, as the test Reynolds number increased, various adverse effects such as tunnel turbulence, the reduction in boundary-layer stability and surface contamination led to increasingly patchy behavior both chordwise and spanwise on the test articles.

Drag Characteristics

The drag of the airfoil sections was measured using a traversing wake rake with probes at four spanwise stations, (Fig. 7). As the probe nearest the tunnel wall showed some wall effects, its output was not used. In tests of the airfoils

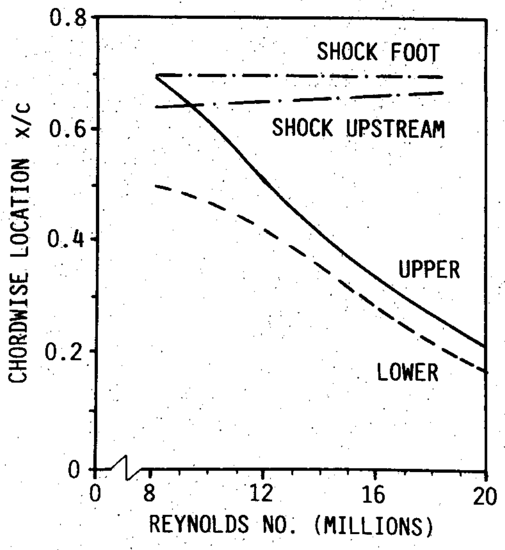

Fig. 6 Sixteen percent thick airfoil chordwise location of start of transition at $M=0.74$–0.76; $C_L=0.6$.

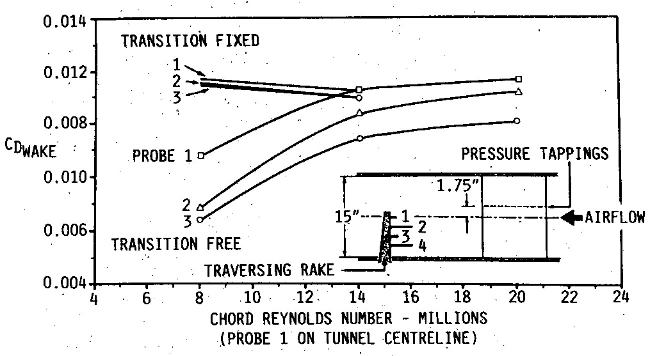

Fig. 7 Sixteen percent thick airfoil spanwise drag variations for $M=0.74$; $C_L=0.6$.

with transition fixed the other three probes showed very similar drag values (Fig. 7), indicating good spanwise uniformity in the tunnel flow. In contrast, the tests with transition free showed spanwise variations in drag indicative of varying amounts of laminar flow ahead of each probe. In the case of the 16% airfoil, probe 1 gave consistently higher drag values, which may be caused by the wake spreading from the transition wedge in the pressure tapped region (Fig. 7). Accordingly, the section drags were finally based on averages of the values from probes 2 and 3 only. In the case of the 21% airfoil, the averaging was based on probes 1 and 3 as the pressure taps were in line with probe 2 for that installation.

Typical drag polars for the two airfoils with NLF are shown in Fig. 8, at a Reynolds number per foot of 8 million and a Mach number of 0.75 for the 16% airfoil and $M=0.68$ for the 21%. Both airfoils achieved minimum drag coefficients, $C_{D\min}$, of about 0.005, while the best lift/drag ratios were 109 for the 16% airfoil and 103 for the 21%. In the case of the 16% airfoil the best lift/drag ratio of 109 occurred at the design lift coefficient of 0.6. The 21% thick airfoil showed some partial loss in NLF above a C_L of 0.4, and the best lift/drag ratio of 103 was achieved at a higher lift coefficient about 0.8. Figure 9 shows the 21% airfoil had developed slightly adverse pressure gradients on its upper surface at lift coefficients about 0.6 at $M=0.68$, reducing the airfoil's ability to sustain extensive NLF and accounting for the behavior noted in Fig. 8.

The effects of increasing Reynolds number on the drag of the airfoils are presented in Fig. 10 for the design lift coeffi-

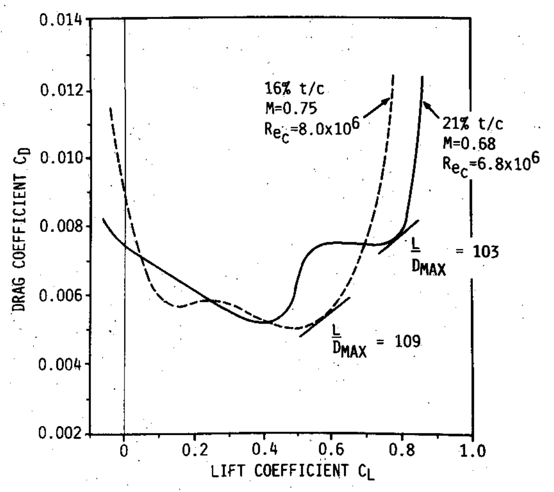

Fig. 8 Drag polars for 16 and 21% thick airfoils with NLF conditions.

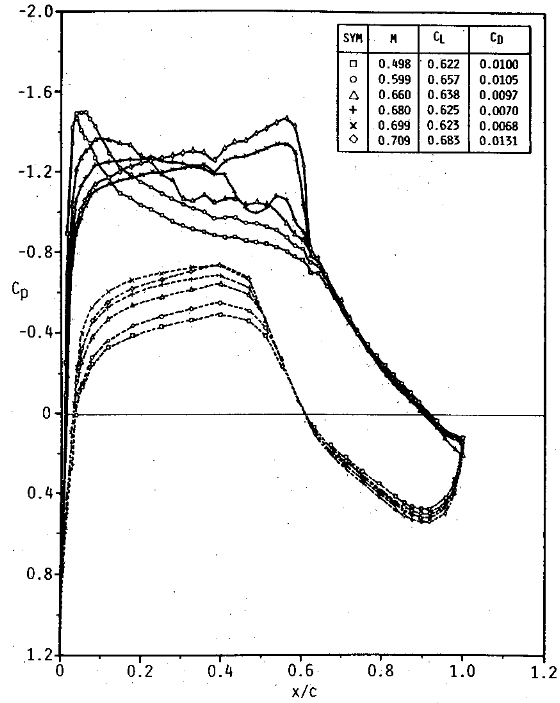

Fig. 9 Effect of increasing Mach number on C_p distribution of 21% t/c airfoil; Re/ft = 8 million.

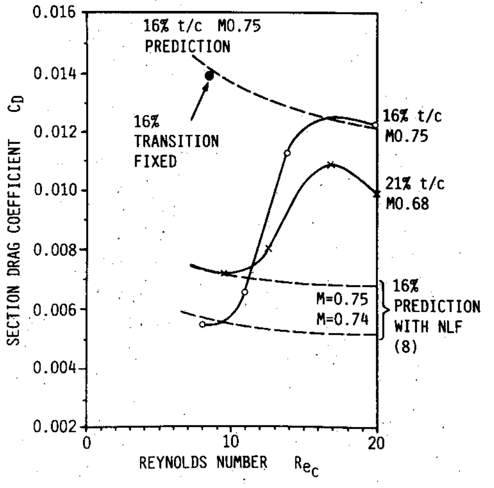

Fig. 10 Influence of Reynolds number on section drag at $C_L=0.6$ with free transition.

cient of 0.6, again at a Mach number of 0.75 for the 16% airfoil and at $M=0.68$ for the 21%. In the case of the 16% thick airfoil the drag coefficient at a Re_c of 8 million was 0.0055 but NLF was rapidly lost above a Re_c of 11 million and drag increased progressively. The flow visualization had shown that fully turbulent behavior was established by a Re_c of 20 million, and the corresponding drag coefficient of 0.0122 was 2.2 times the NLF drag value obtained at a Re_c of 8 million. The behavior of the 21% thick airfoil was similar in character but the drag increase was less and delayed to slightly higher Re_c. The 16% thick airfoil demonstrated a much larger drag increase with increasing Reynolds number, and this was because it progressed more deeply into drag rise at the Mach numbers used for this particular comparison.

The drag estimated for the 16% airfoil at $M=0.75$ is included in Fig. 10, as predicted by an extended version of the BGK code. The turbulent airfoil estimates assumed that transition was forced at 10% chord on both surfaces and at a Re_c of 20 million the estimates agreed well with the experiment. The airfoil was also tested with transition fixed at a Re_c of 8 million and the associated drag value included in Fig. 10 also shows good agreement with the estimates.

The pressure distribution about the 16% airfoil at conditions for NLF is given in Fig. 11 and it shows the Mach number upstream of the shock was about 1.24. Based on BGK calculations this would correspond to an increment due to wave drag of about C_d of 0.002, and given the measured section drag of 0.0055 indicates the skin friction drag component was only about a C_d of 0.0035.

The NLF drag predictions shown in Fig. 10 used the method of Cebeci, Mosinskis, and Smith,[8] and this indicated extensive laminar flow should be maintained to Re_c beyond 20 million, which was not found to be the case in the tests. Transition predictions were also made with the method of Van Driest and Blumer,[2] which allowed the effects of freestream turbulence on transition to be evaluated. Even when the assumed turbulence levels were set to zero, this method predicted transition at Re_c much lower than observed in practice, suggesting it was unduly pessimistic.

The drag measured with NLF at Mach 0.75 and Re_c of 8 million was lower than predictions, and it was found the drag predicted for Mach 0.74 actually gave better agreement with the value measured at Mach 0.75 (see Fig. 10). This discrepancy occurred because the airfoil code predicted the shock to be further back and stronger than found experimentally, which in turn caused the onset of drag rise to be shifted to lower Mach numbers. An experimental pressure distribution about the 16% t/c airfoil with NLF ($M=0.75$ $Re_c=8$ million), is compared with the predicted pressure distribution for a lower Mach number of 0.74 in Fig. 11. The chordwise locations of the shocks and their strengths become very similar, which suggests that NLF predictions using the DHC/NAE/BGK code must use a Mach number about 0.01 lower than test in order to match experimental pressure distributions and drag values. In addition, Fig. 11 shows that the measured pressure gradients on the upper surface were flatter than the estimates, which should have caused transition to occur earlier than predicted. The discrepancies found with NLF conditions suggest that further theoretical work is

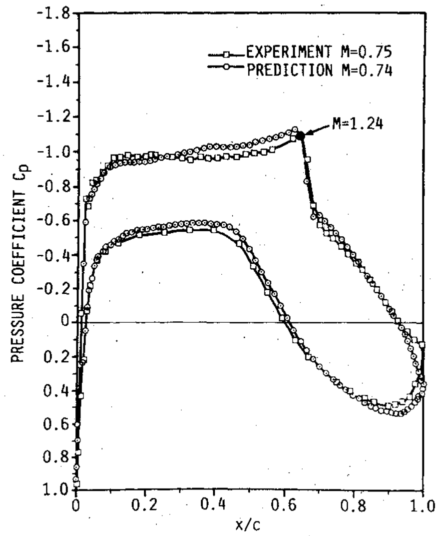

Fig. 11 Comparison of measured and predicted C_P distributions on 16% airfoil $C_L=0.6$; Re/ft = 8 million; transition free.

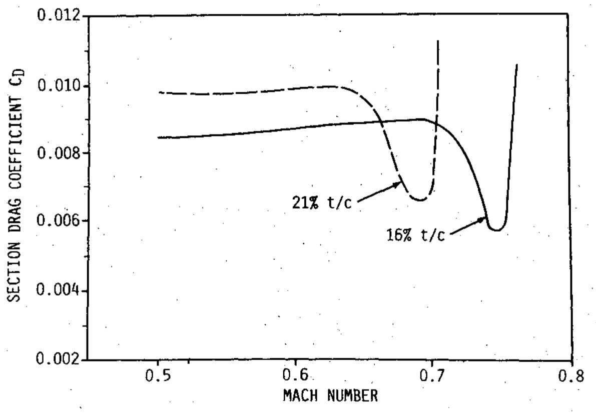

Fig. 12 Influence of Mach number on drag of 16 and 21% t/c airfoils with NLF Re/ft = 8 million and $C_L=0.6$.

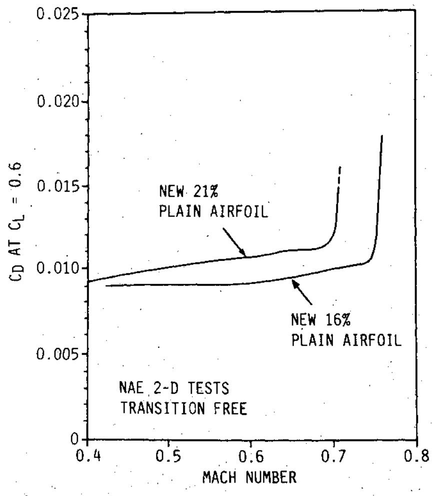

Fig. 13 Drag characteristics of new supercritical airfoils at high Reynolds numbers.

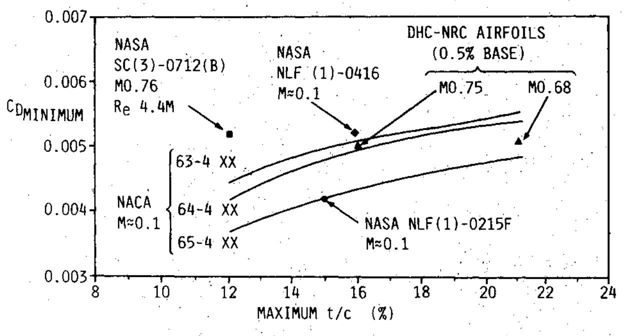

Fig. 14 Comparison of NLF airfoil minimum drags at Reynolds numbers about 8 million, transition free.

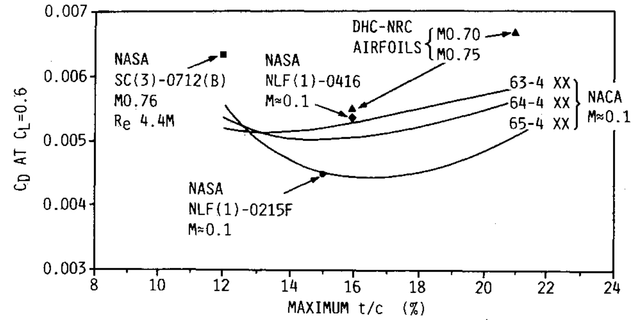

Fig. 15 Comparison of NLF airfoil drags at $C_L = 0.6$ and Reynolds numbers about 8 million, transition free.

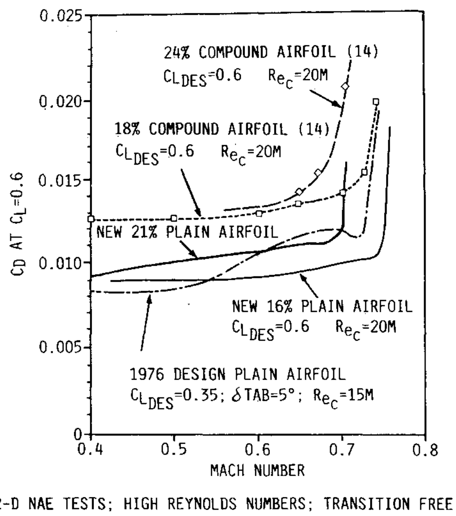

Fig. 16 Comparison of drag characteristics of unblown supercritical airfoils.

needed on modeling the shock wave interaction with laminar boundary layers.

The influence of increasing Mach number on the drag coefficients of the two airfoils at the design lift coefficient of 0.6, for conditions supporting NLF (*Re*/ft of 8 million, transition free) is shown in Fig. 12. Both airfoils exhibited a deep bucket in their drag curves, centered about $M = 0.74$ in the case of the 16% airfoil and about $M = 0.69$ for the 21% airfoil. There was a narrow spread of Mach numbers over which the drag reductions due to NLF were most significant, suggesting that a variable airfoil geometry may be needed for successful exploitation of this effect over a wider range of Mach numbers.

The variation of drag coefficient with Mach number at high Reynolds numbers where behavior was fully turbulent, is shown in Fig. 13. Both of the new airfoils showed very little drag creep and the 16% airfoil demonstrated a drag rise Mach number, M_{dr}, of 0.75 while the 21% airfoil achieved 0.69.

Comparisons with Other Airfoils

At the present time there is very little published data on NLF airfoils at supercritical conditions so most comparisons have to be made with low speed airfoil test data. NASA has recently developed two modern low speed NLF airfoils designated NLF(1)-0416,[9] and NLF(1)-0215(F),[10] which were tested in the low turbulence wind tunnel at Langley. There is also the earlier NACA work on the 64, 65, and 66 series of NLF airfoils reported in Ref. 11. Recent NASA tests in the 0.3m cryogenic tunnel at transonic conditions provide some data on a 12% thick supercritical airfoil[12] and a 10% airfoil,[13] but these airfoils only displayed NLF behavior at lower Re_c (about 4.4 million) than the NRC tests reported herein.

The minimum drag coefficients, $C_{d_{\min}}$, of the various airfoils with conditions giving NLF are given in Fig. 14, while Fig. 15 compares their drag data for a lift coefficient of 0.6. Bearing in mind that the drag of the DHC/NRC supercritical airfoils includes some wave drag, that the airfoils have blunt trailing edges and that the lower surfaces have incomplete laminar flow, the drag values achieved appear commendably low.

The variation of drag with Mach number for the new airfoils at high Reynolds numbers giving near fully turbulent flow, is compared in Fig. 16 with three other thick, supercritical airfoils tested previously in the NAE facility. The 1976 "plain" airfoil was originally designed for a lift coefficient of 0.35 but it was recambered with 5 deg of flap deflection to improve its performance at higher lift. The second comparison is made with two unblown "compound" airfoils of 18% and 24% thickness designed for a lift coefficient of 0.6.[14] The new airfoils show substantial improvements in their levels of drag and in their drag rise Mach numbers relative to the previously tested airfoils. Comparisons made with a wide range of other supercritical airfoils tested in the NAE facility show the new airfoils to be equal to or superior to the best examples.

Conclusions

Based on the work to date on NLF-capable airfoils the following can be concluded.

1) It was found possible to demonstrate extensive NLF on airfoils at chord Reynolds numbers of at least 11 million in the NAE facility used for these tests.

2) The design features needed for airfoils to have good characteristics with turbulent boundary-layers can be reconciled with good NLF capabilities for the range of thicknesses investigated.

3) The discrepancies observed between drag predictions and test values for cases with NLF show the need to improve methods, possibly in the areas of shock wave/laminar boundary-layer interaction and also for boundary-layer transition prediction in the presence of turbulence, roughness, and noise.

Acknowledgments

The authors wish to acknowledge the valuable contributions made by F.C. Tang (NRC/NAE) and I.G. Fejtek (DHC) in the wind-tunnel testing, data reduction, and reporting for these investigations. This R&D was jointly supported by the de Havilland Aircraft Company of Canada (DHC), a Division of Boeing of Canada Ltd., Downsview, Ontario, Canada, and by the PILP Office of the National Research Council of Canada (NRC).

References

[1]Elfstrom, G.M., "Skin Friction Measurements on Two Relatively Thick Airfoil Sections at High Reynolds Numbers," NRC/NAE Aero Note NAE AN23, Nov. 1984.

[2]Van Driest, E.R. and Blumer, C.B., "Boundary Layer Transition: Freestream Turbulence and Pressure Gradient Effects," *AIAA Journal*, Vol. 1, June 1963, pp. 1303–1306.

[3]Fancher, M.F., "Aspects of Cryogenic Wind Tunnel Testing at Douglas," AIAA Paper 82-0606, 1982.

[4]Bauer, F., Garabedian, P., and Korn, D., *Supercritical Wing Sections III*, Lecture Notes in Economics and Mathematical Systems, Springer-Verlag, New York, 1977.

[5]Eggleston, B., Jones, D.J., and Elfstrom, G. M., "Development of Modern Airfoil Sections for High Subsonic Cruise Speeds," AIAA Paper 79-0687, March 1979.

[6]Ohman, L. H., Brown, D., and Bowker, A. J., "Recent Improvements to The NAE 5 Ft × 5 Ft Blowdown Wind Tunnel," Aero Note NAE-AN-31, NRC 24882, Aug. 1985.

[7]Jones, D.J. and Khalid, M., "Analysis of Experimental Data for a 21% Thick Natural Laminar Flow Airfoil, NAE 68-060-21:1,"

Aero Note NAE-AN-34, NRC 25076, Oct. 1985.

[8]Cebeci, T., Monsinskis, G.J., and Smith, A.M.O., "Calculation of Viscous Drag and Turbulent Boundary Layer Separation Two-Dimensional and Axisymmetric in Incompressible Flows," Rept. MDCJ0973-01, Douglas Aircraft Co., 1970.

[9]Somers, D. M., Design and Experimental Results for a Natural-Laminar-Flow Airfoil for General Aviation Applications," NASA TP 1861, June 1985.

[10]Somers, D.M., "Design and Experimental Results for a Flapped Natural Laminar Flow Airfoil for General Aviation Applications," NASA TP1865, June 1981.

[11]Abbott, I.H. and von Doenhoff, A.E., *Theory of Wing Sections,* Dover Publications, New York, 1959, pp. 523–641.

[12]Johnson, W.G., Hill, A.S., and Eichmann, O., "High Reynolds Number Tests of a NASA SC(3)-0712(B) in the Langley 0.3 Meter Transonic Cryogenic Tunnel," NASA TM 86371, June 1985.

[13]Johnson, W.G. and Hill, A.S., "Pressure Distributions From High Reynolds Number Tests of a Boeing BAC 1 Airfoil in the NASA Langley 0.3 Meter Transonic Cryogenic Wind Tunnel," NASA TM 87600, Dec. 1985.

[14]Whittley, D.C., "An Update on the Canada/USA Augmentor-Wing Project," AGARD CP 365, May 1984, Paper 10.